Growth Rates and Morphologies of Miscible PCL/PVC Blend Thin and Thick Films

Vincent H. Mareau and Robert E. Prud'homme*

Department of Chemistry, CERSIM, Laval University, Québec, Canada G1K 7P4

Received July 12, 2002; Revised Manuscript Received November 7, 2002

ABSTRACT: Growth rates and morphologies of thin (0.1−2 μm) and thick (30 μm) films of miscible poly(ϵ-caprolactone)/poly(vinyl chloride) (PCL/PVC) blends have been investigated. Under isothermal crystallization, PCL growth rates decrease in blend films thinner than 1 μm. However, in pure PCL films, no growth rate dependence is seen at the same thicknesses. In thick films of blends isothermally crystallized at a slow growth rate, two types of spherulites are observed with different growth rates and morphologies. One type of spherulites develops at the free surface of the film whereas the other is located in the bulk. The surface enrichment of the blend in PCL appears to be a key factor explaining the crystallization and morphological behavior of this system.

Introduction

As polymer thin films are increasingly used in microelectronic applications,[1] several studies[2−7] have recently been devoted to the crystallization of thin and ultrathin homopolymer films. It was shown that growth rates and morphologies of ultrathin films, i.e., less than 100 nm, are thickness-dependent. Kressler, Wang, and Kammer[2] have observed that the morphology of ultrathin poly(ϵ-caprolactone) films is controlled by the competition between dewetting and crystallization, and that different morphologies are generated as a function of film thickness. Sakai et al.[3] have reported a novel crystalline morphology, called terrace morphology, which develops in thin poly(ethylene terephthalate) films; those terraces, which have a single-crystal-like structure, are 13 nm thick and appear at the periphery of thicker spherulites where the growth front is surrounded by a 2−4 nm thin melt layer. Similarly, Taguchi et al.[4] have shown that 11 nm isotactic polystyrene films exhibit a single-crystal morphology, different from the bulk morphology, with a lateral growth rate decreasing by about 55% when going from the bulk to 11 nm thick films.

Crystallization rates of ultrathin poly(*n*-hexylsilane) films have also been found to decrease with film thickness, below 50 nm, and the crystallinity to decrease for films thinner than 15 nm, for both high and low molecular weight polymers.[5,6] As the number of entanglements and coil dimensions do not explain this reduced crystallinity since there is no molecular weight dependence, it was proposed that the formation of nuclei of critical size might be hindered in the thinnest films. Finally, Dalnoki-Veress et al.[7] have shown that the growth rate of ultrathin poly(ethylene oxide) films slows down for films thinner than 100 nm (with no variation being observed from 1000 to 200 nm), the growth rates of 40 nm films being 3 times smaller than the maximum growth rates observed, at several crystallization temperatures.

Industrial polymers are often made of semicrystalline polymer blends, which are often composed of a semicrystalline polymer and an amorphous one. In this category, the poly(ϵ-caprolactone)/poly(vinyl chloride) (PCL/PVC) blend is a reference system. Its miscibility has been well established,[8−13] and its morphology and kinetics of crystallization have been followed under various conditions.[10,11,14−18] The miscibility of this system is found in the amorphous phase whereas the crystalline phase is made of PCL only.

PCL has a crystal structure close to that of polyethylene, with almost identical *a* and *b* dimensions of its orthorhombic unit cell,[19] and a planar zigzag conformation. However, PCL has a larger *c* parameter than polyethylene due to the presence of the ester group in the hydrocarbon chain. Reported melting temperatures for PCL are close to 60 °C with, for example, a value of 61 °C for the PCL-700 (Union Carbide Corp.) which was studied by a number of investigators.[20] It has been shown that the unit cell dimensions of PCL do not change when blended with PVC,[15] but its melting point decreases and the amorphous interlamellar spacing increases with an increase in PVC concentration.[15,16,21]

In a previous short communication,[22] we reported for a 30 μm thick film of a PCL/PVC blend of 60/40 composition that isothermal crystallization at 40 °C leads to the growth of two types of spherulites: one that develops at the free surface of the film and the other in the core. At the surface of the film, the spherulites develop faster and are coarser than those in the bulk, and they exhibit a lower birefringence. The PCL surface enrichment was pointed out as the probable reason for this behavior.

In this article, the PCL/PVC crystallization behavior observed in ref 22 is expanded and developed with measurements at four different compositions. The influence of the film thickness on the kinetics of isothermal crystallization in thin (100−1000 nm) and thick (30 μm) films is also investigated by bright field and crossed polar optical microscopies for PCL/PVC compositions containing between 80 and 60 wt % PCL and for pure PCL films. Growth rates were measured for thicknesses of about 100, 300, and 800 nm, at crystallization temperatures between 37.3 and 49.5 °C (up to 54°C for pure PCL). Growth rates and morphological measurements were also made in thick films at 40 °C for the 60/40 and 65/35 PCL/PVC compositions, at 44 °C for the

* To whom correspondence should be addressed. E-mail: robert.prud'homme@chm.ulaval.ca.

10.1021/ma0210980 CCC: $25.00
Published on Web 01/07/2003

70/30 and 75/25 PCL/PVC compositions, and at 48 °C for the 80/20 PCL/PVC composition. Correlations between the crystallization behavior of thick and thin films are finally made.

Experimental Section

Materials. Poly(ϵ-caprolactone) (PCL) and poly(vinyl chloride) (PVC) were purchased from Aldrich Chemicals and were used without further purification. Their molecular weight was determined by gel permeation chromatography. For PCL, it was found that $M_n = 39\,000$ and $M_w/M_n = 1.4$, and for PVC, $M_n = 82\,000$ and $M_w/M_n = 1.6$, where M_n is the number-average molecular weight and M_w the weight-average molecular weight. The glass transition temperatures (T_g) of PCL and PVC were found to be −60 and 80 °C, respectively, using a Perkin-Elmer DSC-7 calorimeter at a heating rate of 20 °C/min. The PCL melting point was found to be 60 °C by the same system. To prepare thin and thick films, pure PCL or PCL/PVC blends were dissolved in tetrahydrofuran (THF) for at least 24 h, at room temperature and in the absence of light.

Thick Film Preparation. To prepare thick films, polymer solutions, with concentrations adjusted to the thickness desired, were poured into Petri dishes (diameter 8 cm) in which microscope cover glasses lie flat. For example, to obtain 30 μm thick films, about 0.2 g of polymers (the exact amount is a function of the composition of the blend as PCL and PVC do not have the same density) was dissolved in 50 mL of THF. The solvent was slowly evaporated for at least 5 days. The cover glasses, on which a thick polymer film was deposited, were then carefully removed from the Petri dishes.

Thin Film Preparation. Thin films were prepared by spin-coating at a rotation speed of 3000 rpm during 20 s using a Headway Research Inc. EC101 apparatus. The polymer solutions used for spin-coating were more concentrated than those used for casting thick films. Concentrations from 2.5 up to 8% (g/mL) were used to obtain thicknesses ranging between 100 and 1000 nm. To keep a solvent-saturated atmosphere around the sample and to allow a uniform evaporation, a glass dome was placed on top of the sample area during spin-coating. Film thicknesses were measured by atomic force microscopy.

Atomic Force Microscopy. A Nanoscope III, Dimension 3100, atomic force microscope (AFM) (Digital Instrument) was used to examine the surface topology of thin PCL/PVC films and to determine their thickness. A 90 μm scanner was operated in tapping mode with a standard silicon tip. To determine their thickness, each film was indented with a razor blade and topographic images were recorded by AFM; the thickness of the film was taken as the difference between the height of the film surface (an average made on both sides of the indentation) relative to the surface of the substrate (at the bottom of the indentation). For film thicknesses reaching 1000 nm, the two edges of the cut can be too bulky and exceed the maximum z range of the scanner. To circumvent this problem, measurements were done where the cut starts, scanning in the cut direction; this is the only point where the edges are flat, without a rim.

Optical Microscopy. A Zeiss Axioscop polarizing microscope was used to follow the growth of the spherulites, with a Linkam hotstage, temperature controller, and cooling unit. Microphotographs were recorded with a Toshiba HV-D27 3CCD camera and analyzed with the Image-Pro Plus 4.0 software. Thin and thick samples were melted at 100 °C for 10 min under a nitrogen atmosphere—no coverslip was added on top of the polymer films—and, then, cooled at a rate of 50 °C/min to the crystallization temperature (which was held constant to within ±0.1 °C). Each sample was used only once, at one crystallization temperature. For each sample, the surface of several spherulites, observed in bright field, was measured with the Image-Pro Plus software, for at least 20 microphotographs taken at regular time intervals before impingement. From these surfaces, an average radius was calculated assuming a circular geometry. The radius was then plotted as a function of time, and the slope of these straight lines was calculated ($R^2 \geq 0.999$); this is the average radial growth rate G. Bright field, crossed polar and phase contrast microscopies were used to make morphological observations, during and after isothermal crystallization.

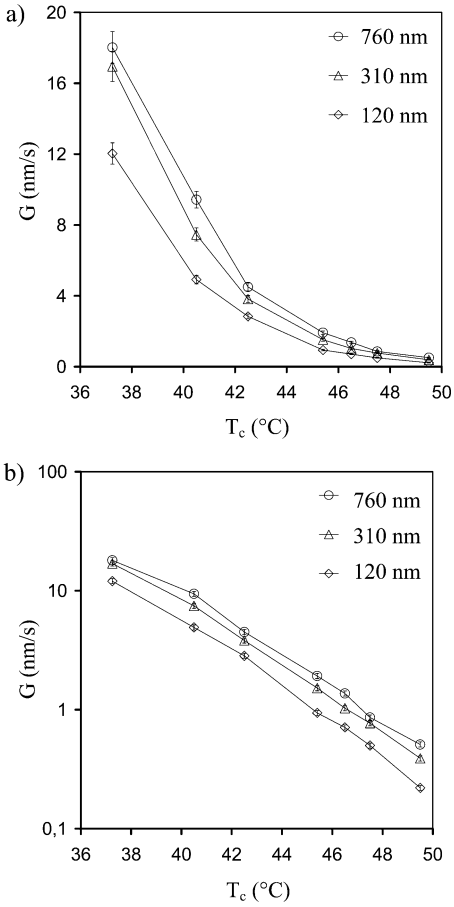

Figure 1. Radial growth rate of a 80/20 PCL/PVC blend as a function of crystallization temperature for three film thicknesses: (a) linear scale; (b) semilogarithmic scale.

X-ray Photoelectron Spectroscopy (XPS). An ESCALAB MKII spectrometer from V.G. Scientific, with a Mg Kα X-ray source, was used to carry out XPS measurements on 30 μm thick films of PCL/PVC blends. The thick films, prepared as described before, were mounted on a standard stub. The X-ray source was run at 15 kV and 20 mA. All spectra were obtained at a takeoff angle of 15° and were curve-fitted using homemade software. Some of the samples described as "upside down" were obtained by removing the polymer film from the glass substrate and carefully depositing it upside down on the substrate. These films stick on the glass substrate due to electrostatic forces only.

Results and Discussion

Thin Films. First, the growth rate of PCL/PVC thin films of 80/20 composition was investigated as this concentration enables observations in a large range of temperatures. Figure 1a shows the growth rate (G) at three different film thicknesses, 120 nm ± 15%, 310 nm ± 12%, and 760 nm ± 12%, in a 37.3−49.5 °C temperature range. For each curve, G decreases with increasing temperature, as expected in this temperature range,[16,23] but the significant decrease of G with the film thickness, particularly visible at lower temperatures, is unexpected for this range of thicknesses (more than 100 nm). As the linear scale of Figure 1a does not allow a clear observation of this phenomenon at high crystallization temperatures because G values are too small, the same data are plotted in Figure 1b using a semilogarithmic scale. It can be seen that the relative

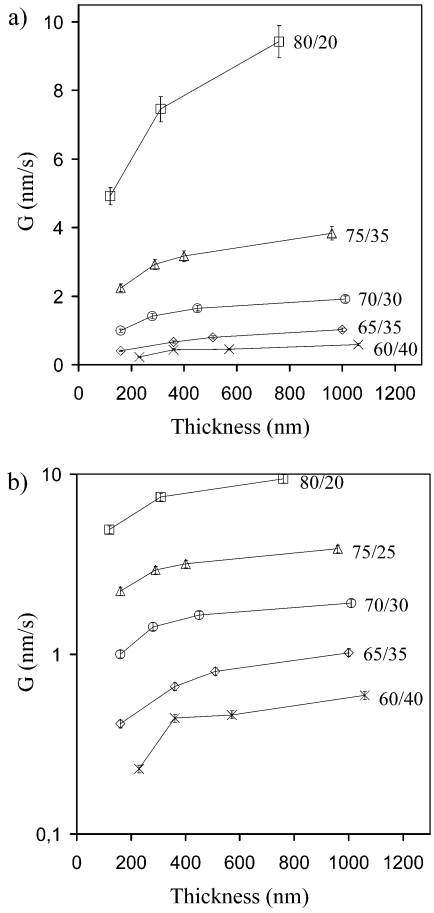

Figure 2. Radial growth rate of five PCL/PVC blends as a function of film thickness, crystallized at 40.5 °C: (a) linear scale; (b) semilogarithmic scale.

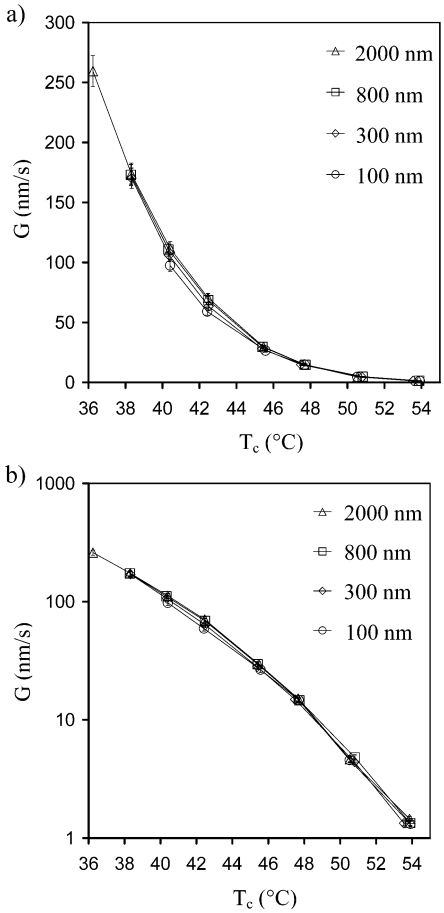

Figure 3. Radial growth rate of pure PCL as a function of crystallization temperature for four film thicknesses: (a) linear scale; (b) semilogarithmic scale.

decrease of G as a function of film thickness is more or less the same at each temperature, and it certainly exceeds the error bars of ±5% on G. The average decrease of growth rate (at the seven temperatures shown in Figure 1a,b) is of the order of 19% from 760 to 310 nm and of 47% when going from 760 to 120 nm. In other words, at this blend composition, thin films with thicknesses of 120 nm crystallize 2 times slower than 760 nm films.

Similar observations were made at 60/40, 65/35, 70/30, and 75/25 PCL/PVC compositions, at a temperature of 40.5 °C, and at four thicknesses ranging roughly from 150 to 1000 nm. Figure 2a shows G values as a function of film thickness for the five compositions, including the 80/20 composition of Figure 1. First, it is seen that G is roughly divided by a factor of 2 each time the PCL content of the blend is decreased by 5%. This is expected from theory[24] since G for a blend is given by

$$G = \nu_1 G_0 \exp\left(-\frac{\Delta E}{R T_c}\right) \exp\left(-\frac{K_G}{f\, T_c \Delta T}\right) \qquad (1)$$

where ν_1 is the volume fraction of PCL in the blend, G_0 a constant that depends of the growth regime, R the gas constant, T_c the crystallization temperature, ΔE the activation energy (necessary for moving crystallizable units through the solid−liquid interface), K_G a constant that depends of the crystallization regime, f a correction factor equal to $2T_c/(T_c + T_f°)$, and ΔT the undercooling, i.e., $T_f° - T_c$. It has also been observed experimentally for many different systems.[25]

Second, as for the 80/20 PCL/PVC composition of Figure 1, G decreases with the film thickness at each composition. To provide a better representation of this phenomenon, the same G data are plotted in Figure 2b on a semilogarithmic scale. For the four new compositions shown in Figure 2, the average growth rate decreases by about 53% when the thickness goes from 1000 to 150 nm, close to the 48% decrease calculated for the 80/20 composition at the same temperature, and the 47% average decrease mentioned above for this blend at seven different temperatures. These data, obtained at different compositions and temperatures, indicate that the decrease of G with the film thickness is a general phenomenon for this polymer blend.

For comparison, the crystallization of pure PCL was also investigated. Figure 3 gives linear (Figure 3a) and semilogarithmic (Figure 3b) plots of G as a function of temperature, at four different thicknesses between about 100 and 2000 nm. It clearly shows that G remains constant within that range of film thickness. However, a closer examination reveals variations exceeding 5% for the 100 nm thick film at the three lowest crystallization temperatures that we were able to monitor (PCL spherulites that grow in 100 nm films at temperatures lower than 40 °C could not be seen by optical microscopy); this average decrease of 12%, when the thickness goes from 800 to 100 nm, for these three temperatures, is still much smaller than those observed for PCL/PVC blends in Figures 1 and 2. It can be explained by the poor optical microscopy resolution and the morphological changes that have been observed in such thin PCL

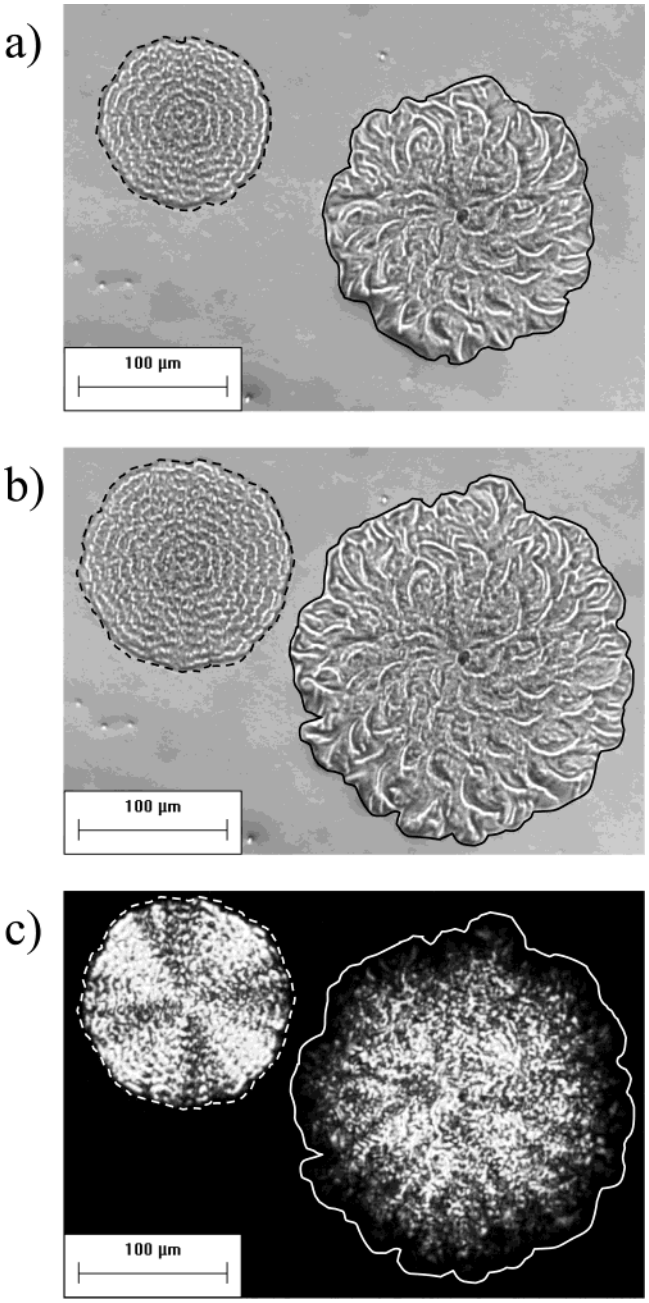

Figure 4. Optical microphotographs of S-type (circled by a full line) and C-type (circled by a doted line) spherulites for a 30 μm thick film of a 75/25 PCL/PVC blend, crystallized at 44 °C: (a) bright field image taken at 15.6 h; (b) idem, same position, 4.5 h later; (c) crossed polar image, same position a few seconds later.

films. (Hedritic morphologies have been observed for 100 nm PCL thin films crystallized at high temperatures.[26])

Thick Films. For comparison, growth rates of thick films of PCL/PVC blends were also investigated. For example, Figure 4 gives optical microphotographs of two neighboring spherulites that develop at different growth rates and with different morphologies in a 30 μm thick PCL/PVC film of 75/25 composition, crystallized at 44 °C. Figure 4a,b was taken in bright field, at the same position in the film, with a time interval of 4.5 h between the two; Figure 4c was taken between crossed polars just a few seconds after Figure 4b, at the same position in the sample. These two spherulites, which are representative of all spherulites observed in that sample, nucleate and develop at different depths in the film. This conclusion can be reached by adjusting the focus of the microscope in bright field and finding that the edges of the spherulites that grow faster are in focus before the edges of the other ones when scanning from the air−polymer interface to the bottom of the film. Therefore, the fast growing spherulites have been labeled S-spherulites (S standing for surface) and the slow growing ones C-spherulites (C standing for core) as these acronyms were already used in the previous paper.[22]

For both types of spherulites, the radius increases linearly with crystallization time[22] as usually observed for spherulitic crystallization (and as observed for the thin films described in Figures 1−3). Growth rates for the spherulites shown in Figure 4 are found to be 1.5 nm/s for the S-spherulites and 0.89 nm/s for the C-spherulites, a difference by a factor of 1.7. Identical samples, crystallized at the same temperature, always give, within an experimental error of ±5%, similar growth rates for the S-spherulites, but more variable results are obtained for the C-spherulites with variations up to ±20%. All the spherulites that develop in the samples are either S-type or C-type, meaning that they exhibit, within experimental error for the S-spherulites and with the kind of variation described above for the C-spherulites, one of the two growth rates reported above and one of the two morphologies described below. No intermediate growth rate, or intermediate morphology, has been found.

In addition to differences in growth rates, different morphological characteristics are associated with the S- and C-spherulites. In Figure 4b, the bright field microphotographs show that the C-spherulite has a compact structure, in contrast to the S-spherulite which has a more open structure. Concentric rings characteristic of banded spherulites can be observed on the C-spherulite whereas large radial fibrils compose the S-spherulite, highlighting a coarser organization. The coarser morphology can also be detected by comparing the wavy growth front of the S-spherulite with the smooth growth front of the C-spherulite.

These observations are confirmed by the microphotograph taken between crossed polars shown in Figure 4c where the C-spherulite exhibits the classical banded Maltese cross pattern characteristic of the spherulitic structure, which has been observed before in the literature for PCL/PVC blends[17,27,28] as well as for many other polymers,[29] whereas the S-spherulite has a more diffuse and slightly less birefringent pattern. It can be noted that the S-spherulite is brighter in its center, with the birefringence decreasing from the center to the edges, but this phenomenon is not observed with the C-spherulite. In view of this, strictly speaking, the word "spherulite" should probably not be used for the S-structure, but we will continue using it for simplicity.

The dual growth rates and morphologies described above for 75/25 PCL/PVC thick films crystallized at 44 °C were also observed at the four other compositions investigated, 60/40, 65/35, 70/30, and 80/20. As the blend was enriched in PCL, it was necessary to increase the crystallization temperature to be able to observe the phenomenon as will be discussed later. Figures 5 is an additional example of dual growth behavior in 30 μm PCL/PVC thick films of 80/20 composition, crystallized at 48 °C. Figure 5b was taken 4.25 h after Figure 5a, and the growth rates of the two types of spherulites were found to be 1.1 nm/s for the S-spherulites and 0.68

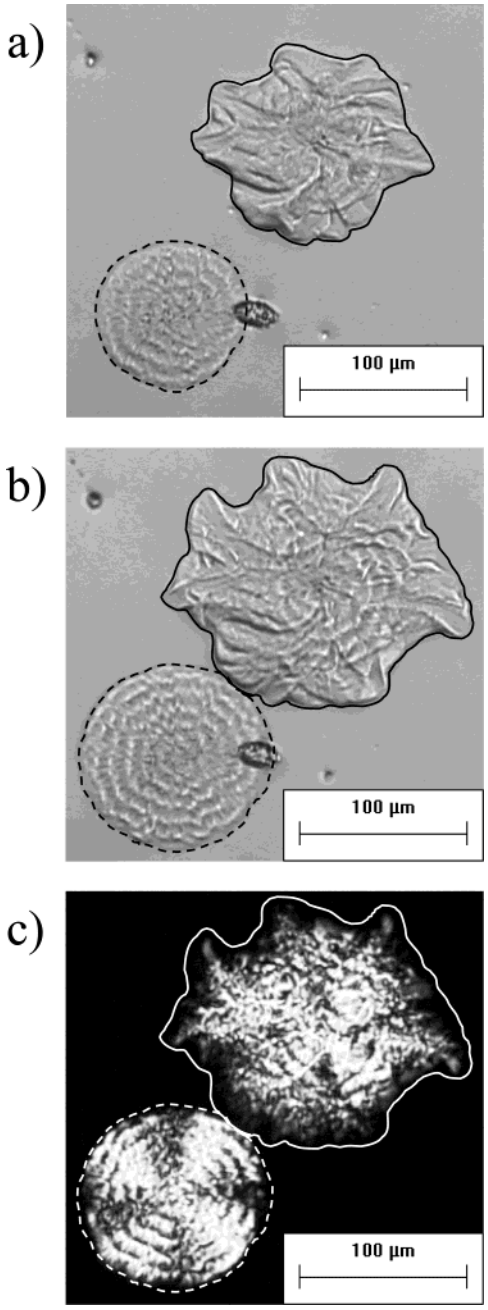

Figure 5. Optical microphotographs of S-type (circled by a full line) and C-type (circled by a doted line) spherulites for a 30 μm thick film of a 80/20 PCL/PVC blend, crystallized at 48 °C: (a) bright field image taken at 23.7 h; (b) idem, same position, 4.25 h later; (c) crossed polar image, same position, a few seconds later.

nm/s for the C-spherulites. For the two compositions illustrated by Figures 4 and 5, the growth rate of the C-spherulites is about 60% slower than that of the S-spherulites, a smaller difference than with the 60/40 PCL/PVC composition where the C-spherulites grow 2−3 times more slowly than the S-spherulites.[22]

As in Figure 4 with the 75/25 PCL/PVC composition, the two types of spherulites of Figures 5 exhibit different morphologies. The S-spherulite exhibits an open structure with wavy edges and no Maltese cross whereas the C-spherulite is circular, with a compact structure and a well-defined banded Maltese cross. The birefringence of the S-spherulite still decreases when moving from the center to the edges. It can, however, be seen that these morphologies are affected by the blend composition and the crystallization temperature. For the C-spherulite, the band spacing increases when the PCL concentration and the crystallization temperature increase, which is consistent with previous observations.[10,17,27] Moreover, the contour of the S-spherulite becomes wavier when going from Figure 4 to Figure 5, and the fibrils become larger. The increase of the crystallization temperature might be responsible for these morphological changes, as Keith and Padden have shown before, but the increase of the PCL content should have the opposite effect. We noticed that the S-spherulites become more birefringent as the PCL content and crystallization temperature increases as seen by comparing the crossed polar optical microphotographs of Figures 4c and 5c, but even more clearly if these two examples are compared to the 60/40 example given in Figure 1c in the previous article.[22] Similar observations were done at the two other compositions.

For each of the five compositions investigated in this work, we observed that, when they meet, C-spherulites keep growing under the S-spherulites, contrary to the usual case for spherulites coming into contact. This phenomenon, briefly described in our previous communication,[22] is more precisely illustrated in Figures 6−8. Figure 6 is composed of six microphotographs taken at the same position on a 30 μm PCL/PVC blend film of 65/35 composition, crystallized at 40 °C. These microphotographs show the growth of two C-spherulites surrounded by S-spherulites at three different times. In each case, bright field and crossed polar microphotographs were taken, one immediately after the other. Figure 6b, a bright field microphotograph, was taken 3.18 h after that of Figure 6a and 4 h before that of Figure 6c. On the left-hand side of the bright field microphotographs, it is possible to see that a S-spherulite is growing on top of a C-spherulite. When looking at the corresponding crossed polar microphotographs, the C-spherulite is seen to develop beneath the S-spherulite. On these microphotographs, none of the two spherulites stops to grow upon contact.

Since the films are 30 μm thick and the spherulites of Figure 6c have an average radius of about 30 μm for the C-spherulites and 75 μm for the S-spherulites, and since there is an overlap between them which is as large as the radius of the C-spherulites (since the S-spherulites reach the center of the C-spherulites), it is impossible for both the C- and S-spherulites to develop like spheres. Even by assuming that the C-spherulite nucleates at the bottom of the film, and the S-spherulite at the free surface, as shown in Figure 7a, the encounter between the two spherulites necessarily creates an asymmetric growth of the C-spherulite. The distance between the spherulites and their radius correspond to the two crystallization times of Figure 6a,c. It can be seen that, with a spherical morphology, the C-spherulite is stopped when meeting the S-spherulite, which results in an asymmetric shape. This is not consistent with the corresponding crossed polar microphotograph that does not show such asymmetry on the banded Maltese cross pattern. Another possibility is that the S-spherulite does not develop like a sphere but more like a cone as proposed before[22] (Figure 3) and as shown here in Figure 7b. In this diagram, which only differs from Figure 7a by the conical shape of the S-spherulite (instead of spherical), we can see that the C-spherulite can nearly grow undisturbed. The conic shape of the

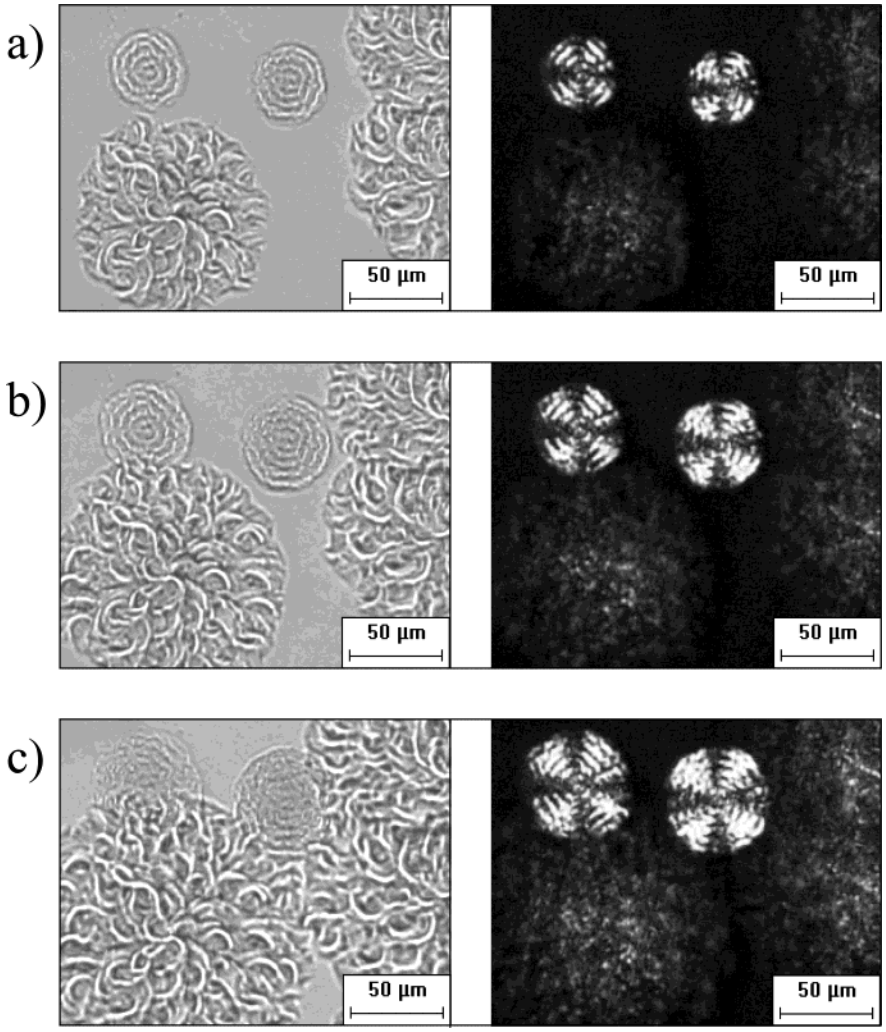

Figure 6. Optical microphotographs of two C-spherulites surrounded by S-spherulites for a 30 μm thick film of a 65/35 PCL/PVC blend crystallized at 40 °C in (a) bright field image taken at 19.42 h and crossed polar image taken a few seconds later at the same position; (b) idem, same position, 3.18 h later; (c) idem, same position, 4 h later than (b).

S-spherulite was generated by making the assumption that the growth rate in the *z*-direction of the film is identical to the growth rate of the C-spherulite, i.e., 3.5 times slower than the radial growth rate of the S-spherulite at the surface. This difference can be explained by a PCL surface enrichment, as it is proposed below. The presence of a conic shape is supported by observations made in both bright field and crossed polar microscopy for S-spherulites. It would also explain why the birefringence of the S-spherulite in crossed polar microphotographs decreases from the center to the edges by a decrease of the thickness of the S-spherulite along that direction.

Another observation that also leads to the conclusion that the thickness of the S-spherulite is really thin on their edges is given in Figure 8. This figure is made of six microphotographs, all taken at the same position on a 30 μm 70/30 PCL/PVC blend film, crystallized at 44 °C. These microphotographs were taken at two different times (t_1 and t_2) of the crystallization process, with a time interval of 8.75 h between them. At each time, three microphotographs were taken almost simultaneously (with just a few seconds between each of them) in bright field with the focus on the core of the sample (Figure 8a), in bright field with the focus on the surface of the sample (Figure 8b), and between crossed polars with the focus on the core of the sample (Figure 8c). The different focus positions allow seeing better the S-spherulite when the focus is on the surface and the C-spherulite when the focus is on the core. (The fibrils of the S-spherulite are seen in one case and the bands of the C-spherulite in the other.) When the two spherulites overlap at t_2, it is still possible to distinguish the edges of the C-spherulite when focusing on it, which indicates that the S-spherulite is thin on top of the C-spherulite. (Otherwise, it would not be possible to see underneath.) It can also be seen that the growth of the S-spherulite is stopped on top of the C-spherulite, as indicated by the arrow in Figure 8b. A diagram similar to that of Figure 7 was drawn, respecting the dimensions shown in Figure 8, to generate the overlap that can occur just before the S-spherulite meets the C-spherulite at the surface. A 10 μm overlap was then found which is close to that observed in Figure 8 (around 12 μm).

Fully crystallized thick PCL/PVC films then exhibit C-spherulites dispersed into a matrix of S-spherulites, as C-spherulites stop growing below S-spherulites when the two different types of spherulites meet in the core of the film. These observations exclude the possibility that S-type spherulites would develop only at the surface of the thick films, not growing in the *Z*-direction, and lead to the probable conic shape of the S-spherulites.

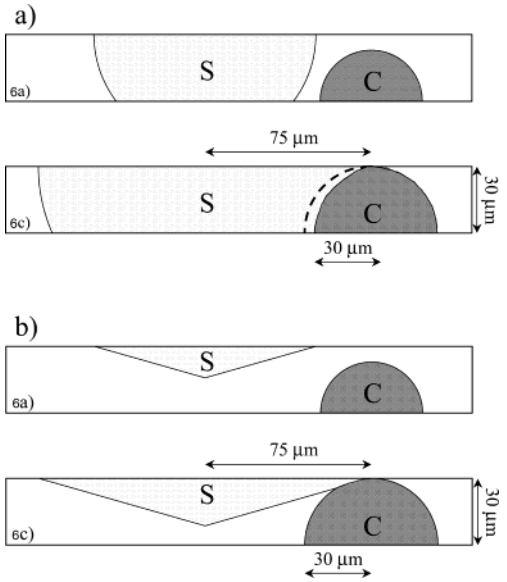

Figure 7. Two schematic cross-section diagrams of the two spherulites illustrated in Figures 6a and 6c, S standing for the S-type spherulite and C for the C-type: (a) the S-spherulite and the C-spherulite are represented with a spherical shape, leading to a truncated C-spherulite; (b) conic geometry for the S-spherulite, leading to a nearly undisturbed growth of the spherical C-spherulite.

Discussion

To explain the above-mentioned results, thick films containing both S- and C-spherulites were analyzed by X-ray diffraction. They all showed peaks corresponding to the *d* spacings of the 110 and 200 reflections of pure orthorhombic PCL, as reported by Bittiger et al.[30] It is thus clear that the two different morphologies observed in the thick PCL/PVC films described in this work are made of the same crystal structure.

We then verified whether there is a PCL surface enrichment in those samples. XPS measurements were carried out on 30 μm PCL/PVC films and on the pure homopolymers. Using C_{1s}, Cl_{2p}, and O_{1s} XPS spectra, atomic chlorine and oxygen concentrations were determined at the top 21 Å surface of the films (which is the sampling depth for the C_{1s} photoelectrons at a takeoff angle of 15° [31]). As some oxygen contamination was observed, only the atomic chlorine concentration was used to determine the weight composition of the PCL/PVC blends at the surface of the thick films, as chlorine is present in PVC but not in PCL.

The results are summarized in Table 1 where weight percent of PCL and PVC detected at the surface is given for two blend compositions and for four different preparation conditions. From these data, it can be seen that there is, in all cases, an important PCL enrichment at the film surface which is exposed to the air during the solvent casting. The top 21 Å of the films is nearly composed of pure PCL, with an average of 97 and 99% PCL for the 75/25 and 60/40 PCL/PVC films, respectively. No significant difference is observed between the solvent-casted films and films that were melted (after solvent casting) and isothermally crystallized.

Some samples were then turned upside down and XPS analyzed. The results show that the surface that was in contact with the glass substrate during the solvent casting is also enriched in PCL, but slightly less than that in contact with air: 90 against 97% PCL for the 75/25 PCL/PVC blend and 85 against 100% PCL for the 60/40 PCL/PVC blend. However, if the same sample is melted and isothermally crystallized, a PCL surface enrichment similar to that observed at the original air−surface shows up at the air−surface interface, with PCL surface concentrations of 97 and 99% PCL for the 75/25 and 60/40 PCL/PVC films, respectively. Similar results have been obtained on thin films for the 80/20 PCL/PVC blend for thicknesses ranging from 100 to 2000 nm.

These observations confirm the PCL surface enrichment of the blend compositions described in this work, at least for the depth investigated by XPS. It also indicates that this enrichment is larger at the surface that crystallizes freely, which is not in contact with the glass substrate. Clark et al.[32,33] have also reported, using XPS measurements, a PCL surface enrichment at the air−polymer interface of PCL/PVC crystalline blends due to the lower surface tension of PCL as compared to PVC.

Since the growth rate of thin films of PCL/PVC blends has been found to depend on the film thickness (Figures 1 and 2), contrary to the case of pure PCL (Figure 3), it is of interest to compare the growth rates observed for thin and thick PCL/PVC films. Table 2 summarizes the growth rates measured at three PCL/PVC compositions for films crystallized at 48 °C for the 80/20 composition and at 40 °C for the 60/40 and 65/35 compositions. Growth rates of S- and C-spherulites are shown for the thick films and for thicknesses between 100 and 200 nm, and between 800 and 1000 nm, for the thin films.

In all cases, the growth rates of the spherulites that develop in the 100−200 nm films are close to the growth rates of the C-spherulites that develop in the thick films. This is particularly true for the 60/40 and 65/35 PCL/PVC compositions with growth rates of respectively 0.23 and 0.41 nm/s for the thin films against 0.22 and 0.40 nm/s for the C-spherulites, whereas for the 80/20 composition, a value of 0.49 nm/s was found for the thin films as compared to 0.68 nm/s for the C-spherulites. Similarly, the growth rates of the spherulites that develop in 800−1000 nm films are close to the growth rates of the S-spherulites that develop in the thick films with values of 0.59 and 1.0 nm/s for the thin films and of 0.66 and 0.88 nm/s for the S-spherulites for respectively the 60/40 and 65/35 PCL/PVC compositions; again, there is a larger difference for the 80/20 PCL/PVC composition with 0.86 nm/s for the thin films and 1.1 nm/s for the S-spherulites.

These data indicate, on one hand, that the growth rates of the spherulites in the thinnest films considered in this work are not influenced by the enriched layer since they crystallize at a rate which is close to that of the C-spherulites. On the other hand, films with a thickness close to 1 μm are greatly influenced by the PCL surface enrichment since the spherulites found in these films crystallize at a growth rate close to that of the S-spherulites observed in thick films where the PCL surface enrichment is maximum.

However, even if the growth rates of the spherulites in the thinnest films are close to those of C-spherulites, their morphologies are very different. As the thickness of the film decreases, the spherulites develop a more open structure, with an irregular growth front. In simple terms, the morphology of the spherulites found in thin films is close to that of S-spherulites. More specifically, the morphologies of the spherulites developing in 100 and 800 nm thin films are very close, and they are close

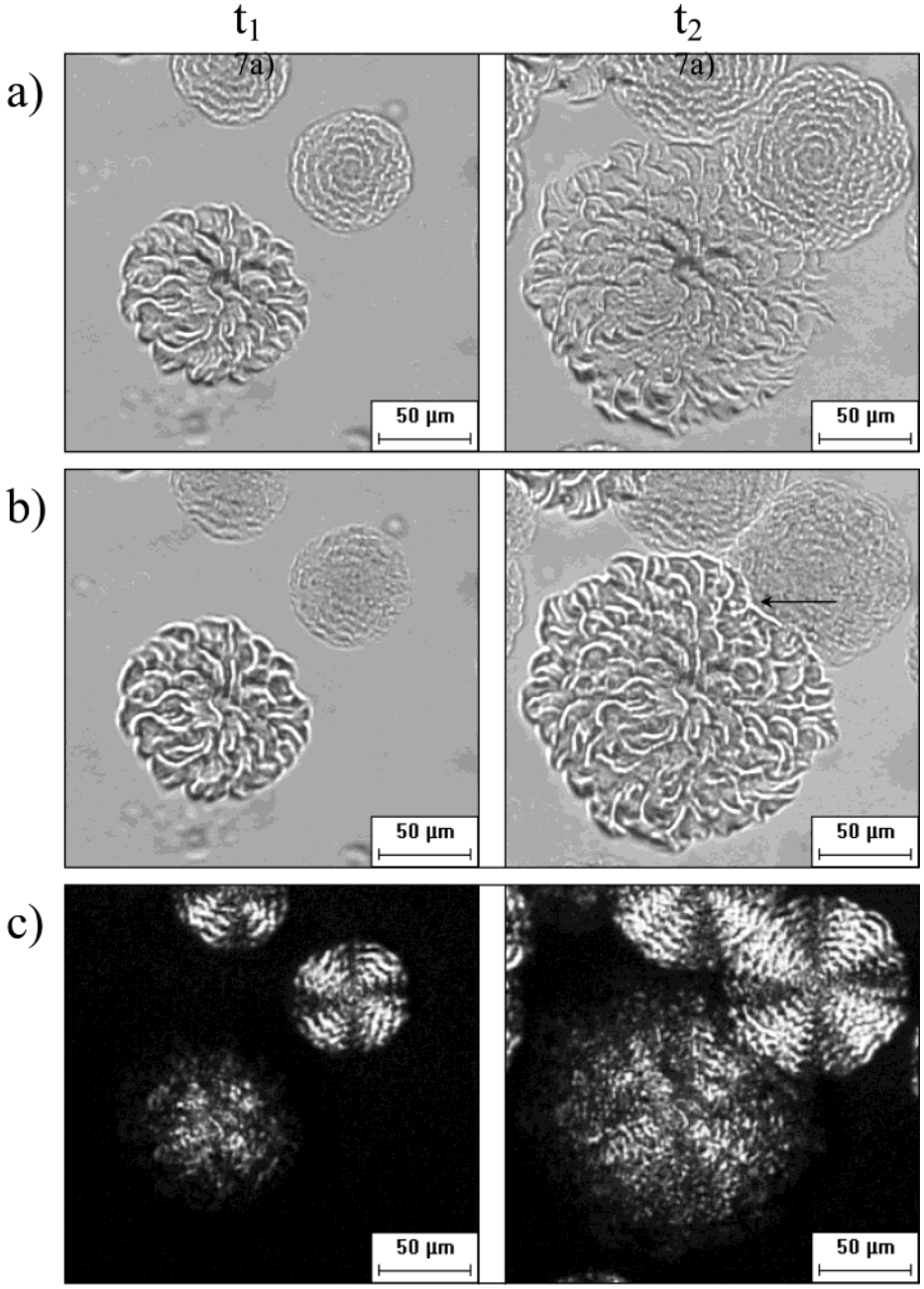

Figure 8. Optical microphotographs of a S-spherulite surrounded by two C-spherulites for a 30 μm thick 70/30 PCL/PVC film crystallized at 44 °C: (a) two bright field images taken at 15.68 h (t_1), and 8.75 h later (t_2) at the same position, with the focus on the core of the film; (b) two bright field images taken a few seconds after t_1 and t_2 at the same position, with the focus on the surface of the film (an arrow indicates where the growth of the S-spherulite stops on the image taken at t_2); (c) two crossed polar images taken a few seconds after t_1 and t_2 at the same position, with the focus on the core of the film.

to that found for the S-spherulites in 30 μm thick samples, even if their difference in growth rate is large. The morphology of the spherulites is then not only controlled by the surface enrichment but also depends on the thickness of the film.

The observation of S-spherulites is more frequent at higher crystallization temperatures where the growth rate is lower. For example, no S-spherulite can be observed in a thick film (30 μm) of 80/20 PCL/PVC composition crystallized at a temperature below 44 °C. For temperatures just above 44 °C, few S-spherulites can be observed, and their texture is not always very distinct from those of C-spherulites. At 48 °C, as illustrated in Figure 6, S-spherulites are clearly seen. When increasing further the crystallization temperature, around 52 °C for example, most of the spherulites that develop in the thick film are S-spherulites. Above 52 °C, at this composition, the growth rate becomes too slow for observation. The limiting temperature, below which S-spherolites are not seen anymore, decreases when the PCL content in the blend decreases, as illustrated by Figure 6 where both C- and S-spherulites are observed in a 30 μm thick film of a 65/35 PCL/PVC blend crystallized at 40 °C.

Obviously, the enriched layer of the polymer blend film is thin, in the nanometer range, as compared to a total thickness of 30 μm. The probability of having a primary nucleus (heterogeneous nucleation) developing in the enriched surface is really small as compared to the probability that it does in the bulk. However, as the surface is enriched in PCL, for a given crystallization temperature, the undercooling is larger at the surface

Table 1. Weight Percent of PCL and PVC Detected by XPS at the Surface of 30 μm Thick Films, for Two Blend Compositions and Four Different Preparation Conditions

	polymer	
thick film	PCL	PVC
75/25, no thermal treatment	97	3
75/25, isothermal crystallization (40 °C)	96	4
75/25, *upside-down*, no thermal treatment	90	10
75/25, *upside-down*, isothermal crystallization (40 °C)	97	3
60/40, no thermal treatment	100	0
60/40, isothermal crystallization (40 °C)	98	2
60/40, *upside-down*, no thermal treatment	85	15
60/40, *upside-down*, isothermal crystallization (40 °C)	99	1

Table 2. Radial Growth Rates for Three Different Blend Compositions Crystallized at Two Different Temperatures (40 °C for the 60/40 and 65/35 Compositions and 48 °C for the 80/20 Composition), in Thick (C and S-Spherulites) and Thin Film

	composition		
film thickness	60/40	65/35	80/20
thick film (C-spherulite)	0.22[a]	0.40	0.68
thin film (100−200 nm)	0.23	0.41	0.49
thick film (S-spherulite)	0.66	0.88	1.1
thin film (800−1000 nm)	0.59	1.0	0.86

[a] Average of 0.18 and 0.26 units.

than in the bulk due to a decrease of the chemical potential (in the bulk) in the presence of more PVC. This means that the formation of a stable PCL nucleus is more probable at the surface than in the bulk, at least in the temperature range investigated. As the crystallization temperature is decreased, the probability of nucleation in the bulk also becomes substantial and the much larger volume of the bulk as compared to the volume of the surface leads to an overwhelming number of nuclei in the bulk. In comparison, at higher crystallization temperatures, the rate of nucleation in the bulk decreases so much that the relative number of nuclei formed at the surface, despite its small volume, becomes dominant.

When decreasing the thickness of the film, the probability of nucleation in the bulk of the film per unit area also decreases; below a certain limit, no more C-spherulites can be observed. This limiting thickness has been determined, for example, for the 80/20 PCL/PVC composition crystallized at 48 °C, to be around 3 μm. At this temperature and composition, films thinner than 3 μm exhibit just one type of spherulite, with a morphology close to that of the S-spherulites observed in 30 μm thick films; for films thicker than 3 μm, the two kinds of spherulites coexist. This specific behavior is found at every temperature (above the limiting temperature described before) and every composition. However, as the PCL content in the blend decreases for a given crystallization temperature, the number of nuclei in the bulk also decreases, faster than the number of nuclei in the enriched surface (as XPS experiments (Table 1) have shown that 60/40 and 75/25 PCL/PVC thick films exhibit a nearly pure PCL surface). Therefore, a decrease of the PCL content in the blend increases the limiting thickness from which the two types of spherulites can be observed in the same film.

We then envision the origin of the dual growth rate behavior observed as follows: as the presence of PVC slows down the growth rate of PCL spherulites (as shown in Figure 2), the PCL in the enriched surface can crystallize faster than in the core of PCL/PVC films, which could explain, at least in part, the two growth rates observed for thick films. The conic shape of the S-spherulite in Figure 7b is then explained by the fact that the lamellae crystallizing at the surface of the film, in the enriched layer, have a faster growth rate than the lamellae which grow in the core of the film. We have assumed that these "slow" fibrils crystallize at the same growth rate as the lamellae of the C-spherulites, which explains the aspect ratio of the conic S-spherulite shown in Figure 7b.

In the figures shown before, the S-spherulites and the C-spherulites retain their initial morphology when they grow. Even after a long crystallization time, when the crystallization of the S-spherulites occurs in the core of the film, no Maltese cross appears, and similarly, C-spherulite fibrils do not behave differently when reaching the surface, whether by changing morphology or growth rate. These behaviors are not well understood at this moment and are still under investigation. It seems that the primary nuclei (heterogeneous nucleation) appearing at the free surface lead to a different crystallization habit from those found in the bulk due to the PCL enriched layer. This free enriched surface, which is assumed to be just a few nanometers thick, might enable a different lamellar organization which repeats itself over several micrometers when the S-spherulites grow in the direction of the core of the thick films. Similarly, the lamellar organization initiated in the core of the film, giving birth to the C-spherulites, does not change when the C-spherulites reach the enriched surface.

Finally, let us emphasize that huge morphological and kinetic differences are observed between the compact spherulites that develop in pure PCL thick films and the S-spherulites crystallized at the same temperature in PCL/PVC blends. The S-spherulites developing at the surface of PCL/PVC blends are very different from the pure PCL spherulites.

Conclusions

In summary, we found that the growth rate of spherulites that develop in thin PCL/PVC blend films (less than 1 μm) is greatly influenced by the film thickness, but not that of pure PCL. Our observations show that, as the film thickness is decreased below 1 μm, the growth rate also decreases with, for example, 100 nm thin PCL/PVC blend films crystallizing nearly 2 times slower than 800 nm ones, this behavior being independent of the composition of the blend or the crystallization temperature in the ranges here investigated.

We also found that this blend exhibits two different types of spherulites in thick films (30 μm), but only for crystallization temperatures above a certain value which increases with the PCL concentration in the blend. The S-spherulites nucleate at the open surface of the film and develop faster than the C-spherulites that nucleate in the core. The S-spherulites have an open morphology and exhibit a low birefringence whereas C-spherulites are compact and exhibit the classical banded Maltese cross pattern when observed between crossed polars. Several optical microscopy observations (among which the overlap seen when the two types of spherulite meet) have led us to the conclusion that the S-spherulites are probably not spherical but more or less conic.

XPS observations made on thick films have confirmed the presence of an excess of PCL at the surface of the films, which is made of almost pure PCL. This PCL surface enrichment could explain, at least in part, the phenomena here reported.

Acknowledgment. This study was supported by NSERC and FCAR grants. We also acknowledge Dr. Alain Adnot for his help with XPS measurements.

References and Notes

(1) Frank, C. W.; Rao, V.; Despotopoulou, M. M.; Pease, R. F. W.; Hinsberg, W. D.; Miller, R. D.; Rabolt, J. F. *Science* **1996**, *273*, 912.
(2) Kressler, J.; Wang, C.; Kammer, H. W. *Langmuir* **1997**, *13*, 4407.
(3) Sakai, Y.; Imai, M.; Kali, K.; Masaki, T. *J. Cryst. Growth* **1999**, *203*, 244.
(4) Taguchi, K.; Miyaji, H.; Izumi, K.; Hoshino, A.; Miyamoto, Y.; Kokawa, R. *Polymer* **2001**, *42*, 7443.
(5) Despotopoulou, M. M.; Miller, R. D.; Rabolt, J. F.; Frank, C. W. *J. Polym. Sci., Part B: Polym. Phys.* **1996**, *34*, 2335.
(6) Despotopoulou, M. M.; Frank, C. W. *Macromolecules* **1996**, *29*, 5797.
(7) Dalnoki-Veress, K.; Forrest, J. A.; Massa, M. V.; Pratt, A.; Williams, A. *J. Polym. Sci., Part B: Polym. Phys.* **2001**, *39*, 2615.
(8) Koleske, J. V.; Lundberg, R. D. *J. Polym. Sci., Part A-2* **1969**, *7*, 795.
(9) Olabisi, O. *Macromolecules* **1975**, *8*, 317.
(10) Khambatta, F. B.; Warner, F.; Russel, T.; Stein, R. S. *J. Polym. Sci., Polym. Phys. Ed.* **1976**, *14*, 1391.
(11) Russell, T. P.; Stein, R. S. *J. Polym. Sci., Polym. Phys. Ed.* **1983**, *21*, 999.
(12) Prud'homme, R. E. *Polym. Eng. Sci.* **1982**, *22*, 90.
(13) Varnell, D. F.; Moskala, E. J.; Painter, P. C.; Coleman, M. M. *Polym. Eng. Sci.* **1983**, *23*, 658.
(14) Ong, C. Ph.D. Thesis, University of Massachusetts, Amherst, 1973.
(15) Ong, C. J.; Price, F. P. *J. Polym. Sci., Polym. Symp.* **1978**, *63*, 45.
(16) Ong, C. J.; Price, F. P. *J. Polym. Sci., Polym. Symp.* **1978**, *63*, 59.
(17) Keith, H. D.; Padden, F. J., Jr.; Russell, T. P. *Macromolecules* **1989**, *22*, 666.
(18) Chen, H.-L.; Li, L.-J.; Lin, T.-S. *Macromolecules* **1998**, *31*, 2255.
(19) Bittiger, H.; Marchessault, R. H.; Niegisch, W. D. *Acta Crystallogr.* **1970**, *B26*, 1923.
(20) Coleman, M. M.; Zarian, J. *J. Polym. Sci., Polym. Phys. Ed.* **1979**, *17*, 837.
(21) Hubbell, D. S.; Cooper, S. L. *J. Appl. Polym. Sci.* **1977**, *21*, 3035.
(22) Mareau, V. H.; Prud'homme, R. E. *Macromolecules* **2002**, *35*, 5338.
(23) Phillips, P. J.; Rensh, G. J.; Taylor, K. D. *J. Polym. Sci., Part B: Polym. Phys.* **1987**, *25*, 1725.
(24) Runt, J. P. In *Polymer Blends*; Paul, D. R., Bucknall, C. B., Eds.; Wiley-Interscience: New York, 2000; Vol. 1, pp 167−186.
(25) Runt, J. P.; Martynowicz, L. M. In *Multicomponent Polymer Materials*; Paul, D. R., Sperling, L. H., Eds.; Adv. Chem. Ser. No. 211; American Chemical Society: Washington, DC, 1986; pp 111−123.
(26) Mareau, V. H., unpublished data.
(27) Nojima, S.; Tsutsui, H.; Urushihara, M.; Kosaka, W.; Kato, N. *Polym. J.* **1986**, *18*, 451.
(28) Nojima, S.; Watanabe, K.; Zheng, Z.; Ashida, T. *Polym. J.* **1988**, *20*, 823.
(29) Keith, H. D.; Padden, F. J., Jr. *Macromolecules* **1996**, *29*, 7776.
(30) Bittiger, H.; Marchessault, R. H.; Niegisch, W. D. *Acta Crystallogr.* **1970**, *B26*, 1923.
(31) Seah, M. P.; Dench, W. A. *Surf. Interface Anal.* **1979**, *1*, 2.
(32) Clark, M. B., Jr.; Burkhardt, C. A.; Gardella, J. A., Jr. *Macromolecules* **1989**, *22*, 4495.
(33) Clark, M. B., Jr.; Burkhardt, C. A.; Gardella, J. A., Jr. *Macromolecules* **1991**, *24*, 799.

MA0210980